

FRACTAL ANTENNA SYSTEM WITH MIMO CAPABILITIES

Gheorghe MORARIU*, Ecaterina-Liliana MIRON**, Micsandra-Mihaela ZARA*

*"Transilvania" University of Brasov, Romania

**"Henri Coandă" Air Force Academy, Brasov, Romania

Abstract: The article presents a fractal stripline antenna system with MIMO capabilities. It was designed for microwave use and it has wideband properties, a wide directivity chart, low emission power and an average gain over 5 dB.

Keywords: fractal, antenna, directivity, gain, MIMO

1. INTRODUCTION

This article presents a fractal antenna with MIMO capabilities [1][2][3]. This frequency-independent antenna consists of four spiral elements. The paper also presents analytical calculations for the geometry of the antenna, as well as for the electromagnetic properties. These are accompanied by experimental results.



Figure 1 MIMO spiral antenna examples [4],[5]

2. DESIGN AND IMPLEMENTATION

2.1 Circular polarization effect

The design of the antenna is based on four fractal sectors which comprise of Archimedean spiral elements.

The analytical calculation that describes the circular polarisation through a degenerative Archimedean spiral (θ less than 5°) is presented next, starting from the classic spiral relation (1). $r = a + b\theta$ (1)

with r and θ – polar coordinates

$$r = a + b\theta \Rightarrow \theta = \frac{r - a}{b} \quad (2)$$

Considering θ' :

$$\theta' = \frac{r' - a}{b} \quad (3)$$

where

$$r' = k \cdot r \quad (4)$$

$$\text{Thus } \theta' = \frac{k \cdot r - a}{b}.$$

Rearranging:

$$\theta = \frac{r}{b} - \frac{a}{b} \quad (5)$$

and

$$\theta' = \frac{k \cdot r}{b} - \frac{a}{b} \quad (6)$$

By expressing the difference between θ' and θ , the circular polarization effect is emphasized:

$$\theta' - \theta = \frac{r}{b} \cdot (k - 1) \quad (7)$$

where $k-1$ and k are rotation coefficients.

For a very narrow θ , $r \cong a$, the spiral equation thus becoming a circle equation in polar coordinates. In this case, θ is very narrow (5°) and this means that its coordinates are between those of the circle and those of the Archimedean spiral. Therefore, the antenna can combine the functioning of fractal circular and spiral elements, thus widening the emission-reception bandwidth.

Considering a narrow opening angle of π/n ($n \leq 8$ is acceptable) where the radiant field is constant and Φ an arbitrary reception angle (figure 2), The variation of the reception phase is determined as follows:

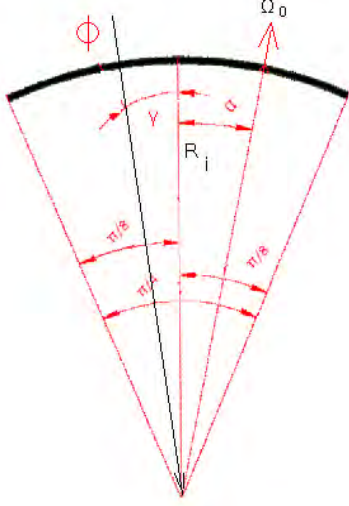


Figure 2 Φ an arbitrary reception angle, Ω_0 the direction of the polar axis and R_i the radius of the i^{th} element

$$\alpha \leq \pm \frac{\pi}{8}, \beta_i = \frac{2\pi}{\lambda_i} \quad (8)$$

$$|A| \cdot e^{j\phi} = e^{j\beta_i R_i} \cdot \sin \theta \quad (9)$$

$$A = |A| \cdot V_i \quad (10)$$

$$V_i = e^{j\phi} \cdot e^{j\beta_i R_i} \cdot \sin \theta_i \quad (11)$$

$$V_i = e^{j(\phi + \beta_i R_i)} \cdot \sin \theta_i \quad (12)$$

For the fascicle: $V_0 = \sum_{i=1}^n V_i = e^{j\phi} \cdot \sum_{i=1}^n e^{j\beta_i R_i} \cdot \sin \theta_i$,

where n is the number of radiant elements.

$$V_0(\Omega) = V_0 \cdot \cos \alpha \quad (13)$$

$V_i V_i$ represents the propagation direction for reception. The θ angle is between V_i and the plane of the antenna surface. V_0 is the total angular phase variation. The expression for reception of E and H waves is:

$$E; H = |E; H| V_0 |E; H| V_0 \quad (14)$$

representing the panoramic reception.

Geometric calculations.

The propagation speed expression is:

$$v = \frac{1}{\sqrt{\epsilon_r}} \cdot \lambda \cdot f \Rightarrow \lambda_{real} = \frac{\lambda}{\sqrt{\epsilon_r}} \quad (15)$$

$$\frac{R_i}{R_{i+1}} = \frac{L_i}{L_{i+1}} \quad (16)$$

where $R_i R_i$ is the radius from the centre to the i^{th} segment of the antenna [6].

$$L_i = \frac{\pi \cdot R_i}{2} = \frac{\pi}{2} \cdot R_i \Rightarrow \frac{\pi}{2} \cdot R_i = \frac{\lambda_{real}}{4} \Rightarrow \lambda_{real,i} = 2 \cdot \pi \cdot R_i \quad (17)$$

$$L_i = \frac{\lambda_{real,i}}{4} \quad (18)$$

$$c = \frac{\epsilon_s}{d}$$

$$S = \sum_{i=1}^6 L_i \cdot \Delta l \quad (19)$$

where S is the total radiation surface for a fractal sector.

$$\lambda_{min} = 2\pi \cdot R_0 \quad (20)$$

$$\lambda_{max} = \sum_{i=1}^6 L_i = \frac{S}{\Delta l} \quad (21)$$

2.2 Antenna design.

The antenna comprises of four fractal spiral sectors which are displayed in axial horizontal and vertical symmetry (figure 4). The geometry of a sector is presented in figure 3 and the distance between the centre and the first spiral element is $R_0 = 24$ mm (distanța de la centru până la primul element fractal spiral). The width of the radiant element is 2 mm and the dielectric width between the radiant elements is also 2mm. Thus the distance from an element to another is 3 mm (for example, $R_5 = 39$ mm and $R_6 = 42$ mm). The antenna was made using a dielectric board with $\epsilon_r = 2.2$, and the thickness $h = 0.8$ mm. AutoCAD 2008 was used for the design.

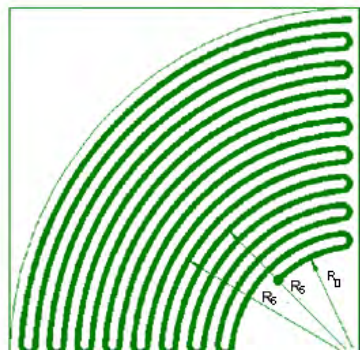


Figure 3 One of the four spiral elements

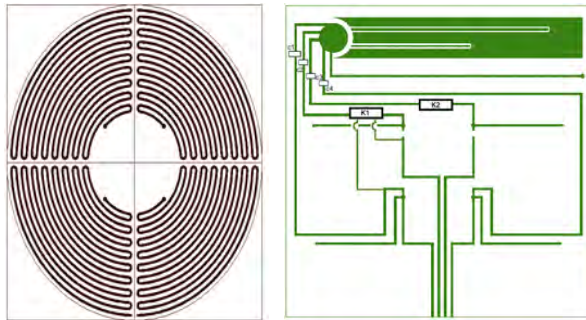
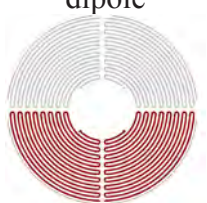


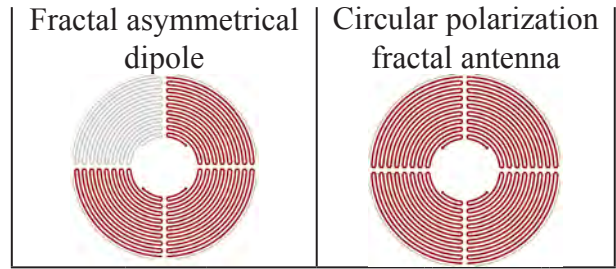
Figure 4 a) the front of the antenna b) the back of the antenna

3. EXPERIMENTAL RESULTS

The MIMO combinations were derived from the structure. The selection of the desired functional combination is made by using the K1 and K2 couplers (figure 5). Table 1 presents the combinations for which the experimental results are provided.

Table 1. Combinations of radiant elements

| Mode | K1 | K2 | Mode | K1 | K2 |
|---|----|----|---|----|----|
| M00 | 0 | 0 | M01 | 0 | 1 |
| Fractal symmetrical dipole | | | Fractal asymmetrical dipole | | |
|  | | |  | | |
| M10 | 1 | 0 | M11 | 1 | 1 |



The measurements were made for a characteristic impedance of 50 Ω.

3.1 VSWR

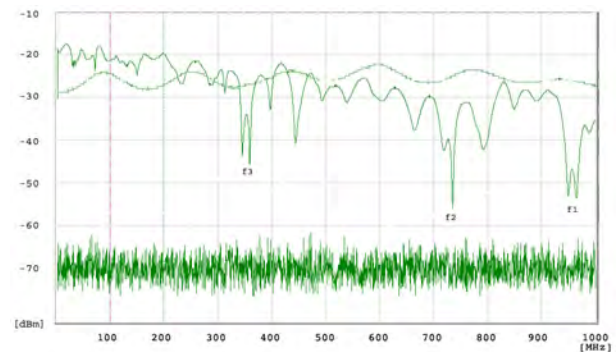


Figure 5 Measured VSWR below 1 GHz

3.2 Simultaneous emission and reception

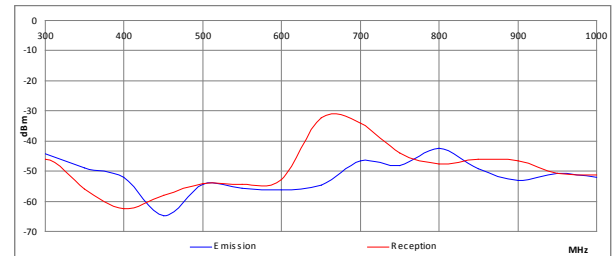


Figure 6 Mode M00 simultaneous emission and reception 300-1000 MHz

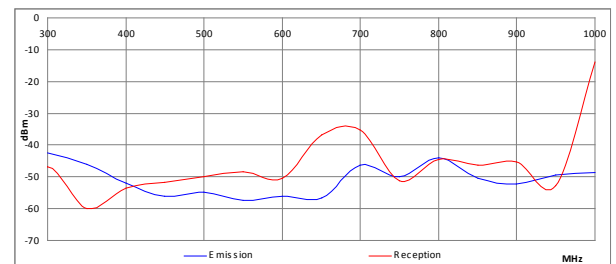


Figure 7 Mode M01 simultaneous emission and reception 300-1000 MHz

Fractal antenna system with mimo capabilities

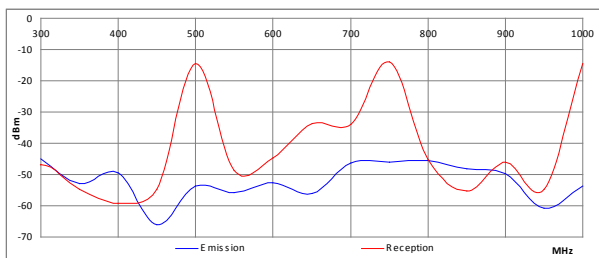


Figure 8 Mode M11 simultaneous emission and reception 300-1000 MHz

3.3 Reception

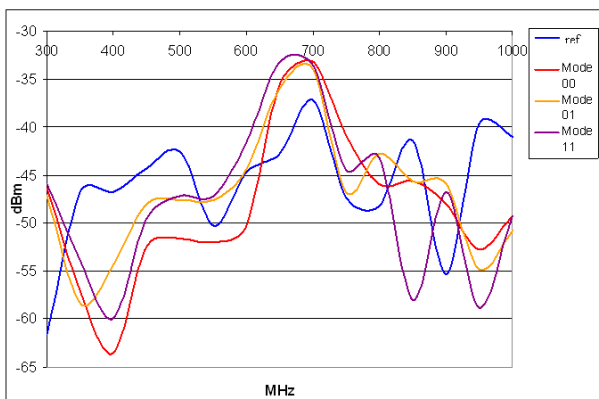


Figure 9 Reception chart 300-1000 MHz for three functional combinations and a reference antenna (blue line, Aaronia HyperLOG 6080)

3.3 Reflection coefficient S11 and the resistance – reactance distribution for the most representative operating bandwidths

Mode 00 as per table 1.

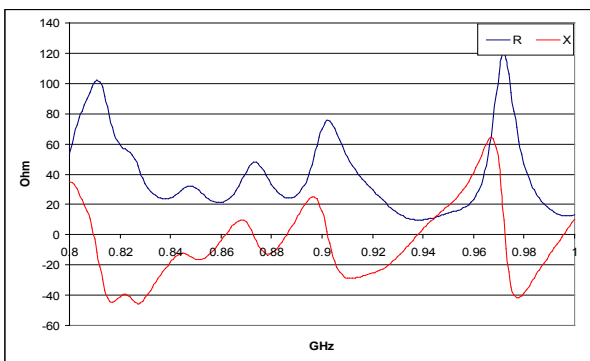
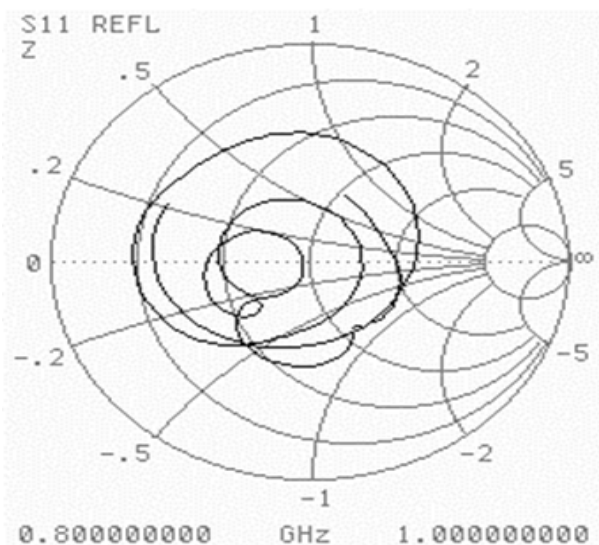


Figure 10 S11 parameter and resistance-reactance distribution for 800-1000 MHz

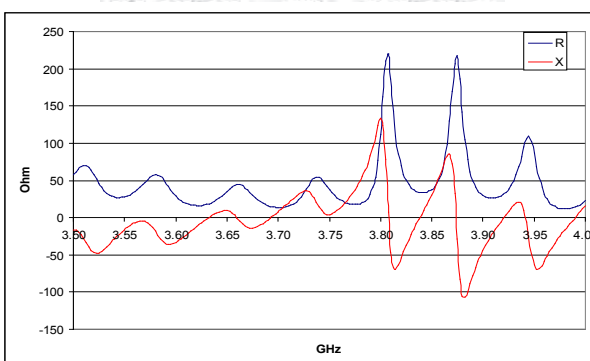
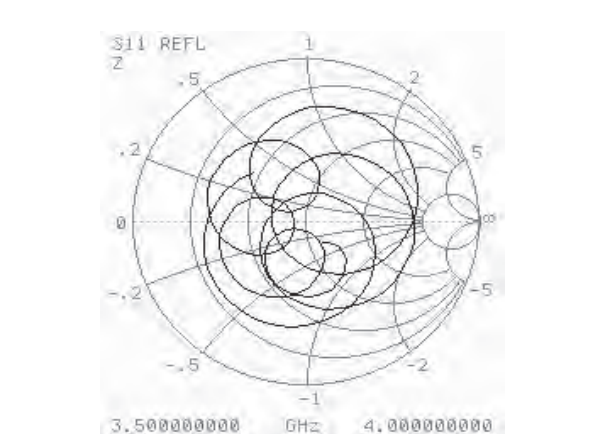
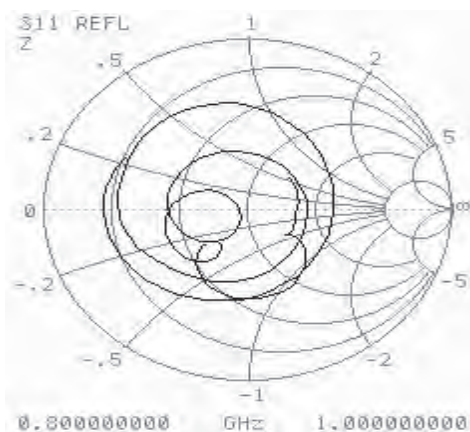


Figure 11 S11 parameter and resistance-reactance distribution for 3.5-4 GHz

Mode 01 as per table 1.



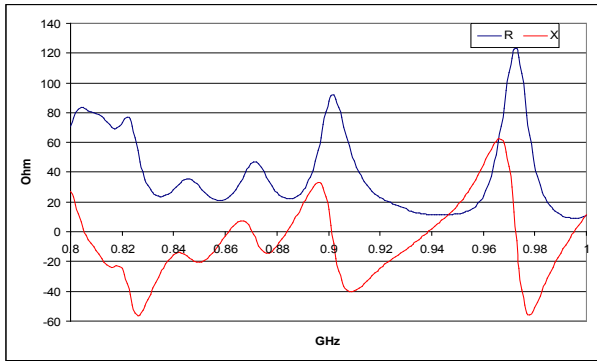


Figure 12 S11 parameter and resistance-reactance distribution for 800-1000 MHz

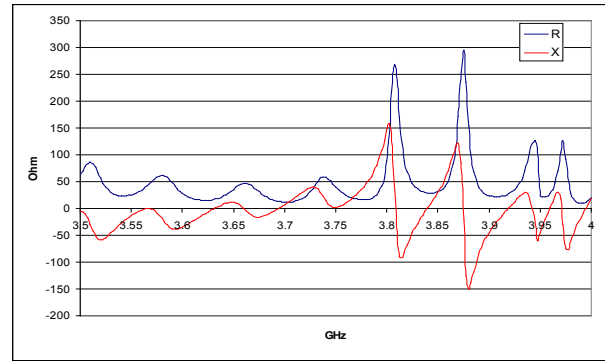


Figure 14 S11 parameter and resistance-reactance distribution for 3.5 – 4 GHz

Mode 11 as per table 1

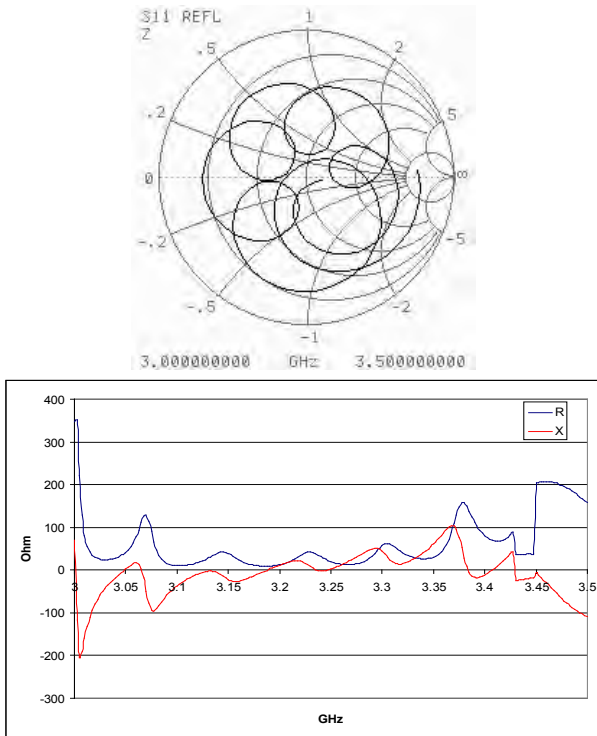


Figure 13 S11 parameter and resistance-reactance distribution for 3 – 3.5 GHz

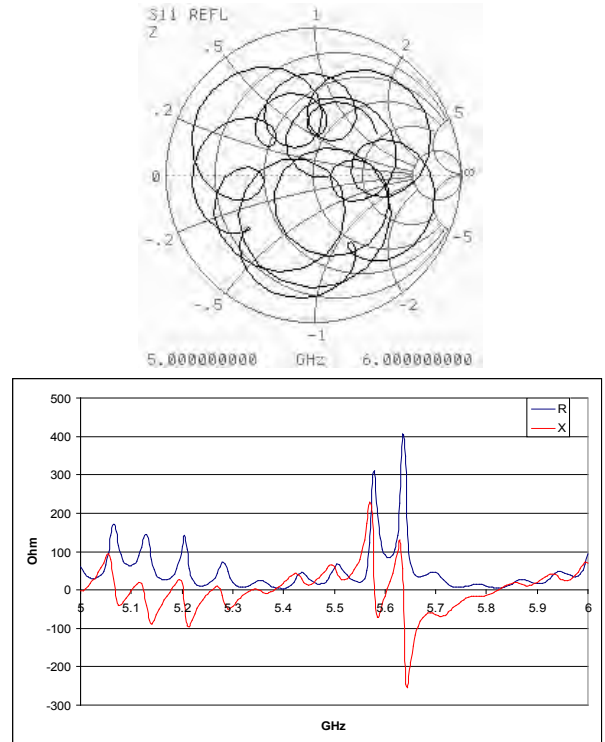
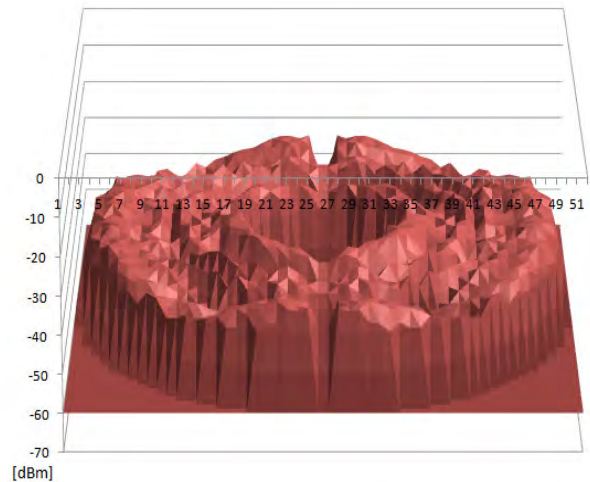
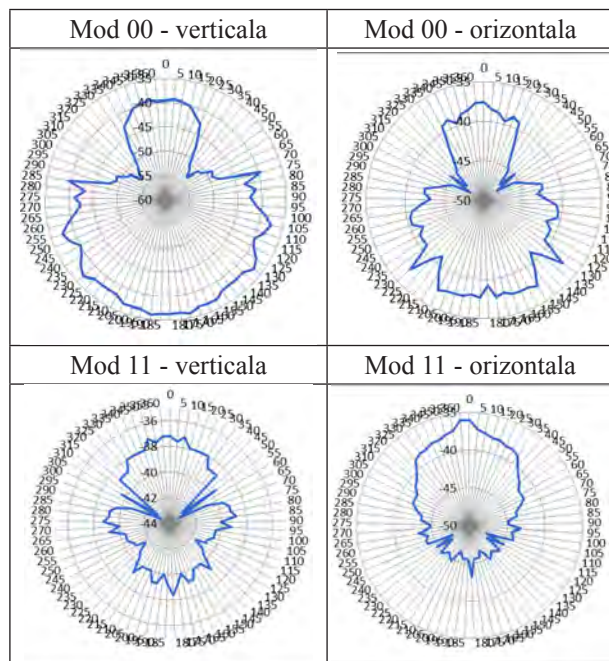


Figure 15 S11 parameter and resistance-reactance distribution for 5 - 6 GHz

3.4 Radiant E field distribution



3.5 Directivity diagram



4. CONCLUSIONS

The next conclusions can be derived regarding the antenna. The antenna has quasi-panoramic reception (following the variation of γ angle—figure 2), an average gain of 5 dB (which is relatively constant) and it is independent of the emission-reception directions (circular polarization).

Its uses range from 4G mobile communications (due to panoramic emission-reception in quadrature architecture) to base stations, wideband emission-reception for communication relays, as well as radio-navigation.

Other advantages stem from it being lightweight and employing a simple manufacturing technology.

One of its disadvantages is a limited emission power, due to its geometrical dimensions. Furthermore, it is not recommended for use in directive antenna systems.

1. http://cdn.rohde-schwarz.com/dl_downloads/dl_application/application_notes/1ma142/1MA142_0e.pdf
2. Gesbert, M. Kountouris, R. W. Heath, Jr., C.-B. Chae, and T. Sälzer, "Shifting the MIMO Paradigm: From Single User to Multiuser Communications," *IEEE Signal Processing Magazine*, vol. 24, no. 5, pp. 36–46, Oct., 2007
3. Ezio Biglieri, Robert Calderbank, Anthony Constantinides, Andrea Goldsmith, Arogyaswami Paulraj, H. Vincent Poor (2010). "MIMO Wireless Communications". Cambridge University Press.
4. Yun-Taek Im, Jee-Hoon Lee, Rashid Ahmad Bhatti, and Seong-Ook Park ,(2008) "A Spiral-Dipole Antenna for MIMO Systems ", *IEEE Antennas And Wireless Propagation Letters*, VOL. 7, 2008 803
5. Nicolaos G. Alexopoulos, Seunghwan Yoon, (2013), „Programmable multiple interwoven spiral antenna assembly”, US Patent 20130010842 A1
6. Morariu Gheorghe; Mailat Marian; Paun Irina Alexandra, (2006) "Microunde: fundamente si aplicatii. Vol. 1 si 2: Linii de transmisie Brasov"; Editura Universitatii Transilvania din Brasov.
7. Nathan Cohen (2002) "Fractal antennas and fractal resonators" U.S. Patent 6,452,553
8. <http://www.antennex.com/preview/vswr.htm>
9. <http://www.tek.com/spectrum-analyzer/h500-sa2500>
10. Shozo Usami and Gentei Sato, "Directive Short Wave Antenna, 1924". *IEEE Milestones*, IEEE History Center, IEEE, 2005.
11. Anritsu 37247E VNA Datasheet